DETECTION AND LOCATION OF STRUCTURAL DAMAGE USING DYNAMIC TEST DATA

ICAS-94-5.8.3

by
O. Sensburg
Deutsche Aerospace, Military Aircraft Division
Munich, Germany

K. Worden and G.R. Tomlinson
Engineering Department, University of Manchester,
Manchester, United Kingdom

Abstract

A method which examines the dynamic behaviour of a structure via undamped normal modes of vibration is presented. A Finite Element (FE) model of the undamaged aircraft is needed. The stiffness matrix of the model is updated using a mathematical optimisation method. The measured mode shapes and modal frequencies of the damaged structure are taken as constraints. Examples are given for a set of damaged metal beams which were analyzed and tested. Defects could be detected and localised by measuring accelerations at only two points.
Damage was also identified also on a carbon fibre fin of a fighter aircraft. In this case, much more mode shape information was needed than for the beams.
A detailed FE-Model of the fin was generated as input for the DASA-Langrange code. A total number of 339 degrees of freedom was used. The mode shapes calculated with simulated defects in the FE-Model were used as constraints. With a sufficient number of points for the first bending mode shape (equal to the number of nodes on the finite element model) detection and localisation of damage was achieved.
Another method which was applied successfully on a simulated cantilever plate is described. This method uses curvatures and neural networks and does not require a finite element description of the structure.
The paper finally discusses measurements taken from a fighter aircraft which show that hydraulic actuators for exciting control surfaces can produce repeatable frequency response functions to extract mode shape information usable for damage detection.

Introduction

Because of safety regulations maintenance of aircraft structures is very costly. Much of that cost is consumed in inspecting aeroplanes at regular intervals (usually, number of flight hours) for structural damage. A structural defect on an aircraft is not monitored and indicated directly like failures of hydraulic and avionic systems. The consumed and remaining life of an aircraft structure can be estimated by recording the loads encountered during flights.
To reduce direct operating of life cycle cost considerable effort has been spent on automated monitoring systems. On-board load monitoring systems for aircraft are already available. These systems do not monitor damage in-situ or on-board. They either indicate loads in excess of design (limit loads) or they accumulate frequently occurring loads (fatigue loads) and compare their damage with analytical predictions or results of a fatigue test. Damage detection still has to be performed manually on the ground by NDT (Non Destructive Test) procedures. These methods cannot readily be applied since a great deal of the aircraft structure is not easily accessible. Fairings, built-in features, equipments have to be removed. Therefore, a large amount of man hours and money is consumed in this effort which, together with repair costs are of the same order as the original acquisition for modern systems. A method which can directly identify structural damage would be highly appreciated by aircraft operators. Two possible candidates for this task are described here.

1. Updating for Detecting Damage

The updating of a finite element model of an aircraft structure with measured vibration modes and frequencies is used to detect and localize damage. The updating is formulated as a classical case of optimisation. The requirements are defined as a general problem of nonlinear programming:

$$f(x) = \min_{x \in R^n}$$

subject to a set of inequality constraints

$$g_j(x) \geq 0 \qquad j=1,m$$

$$x_i^l \leq x_i \leq x_i^u \qquad i=1,n$$

for updating the objective function f(x) as a linear function of the design variables. The design variables x are the cross sectional areas of beam elements, wall thickness for membrane and shell elements, laminate thicknesses for every single layer in composite elements and nodal coordinates. The design constraints g(x) are eigenvalues and eigenmodes of the measured model and the optimization of the structure is performed in an iterative way. Structural defects are found and located by changing the variables x to satisfy the requirements as postulated by measured data with the target function to keep the changes as small as possible (see figure 1).

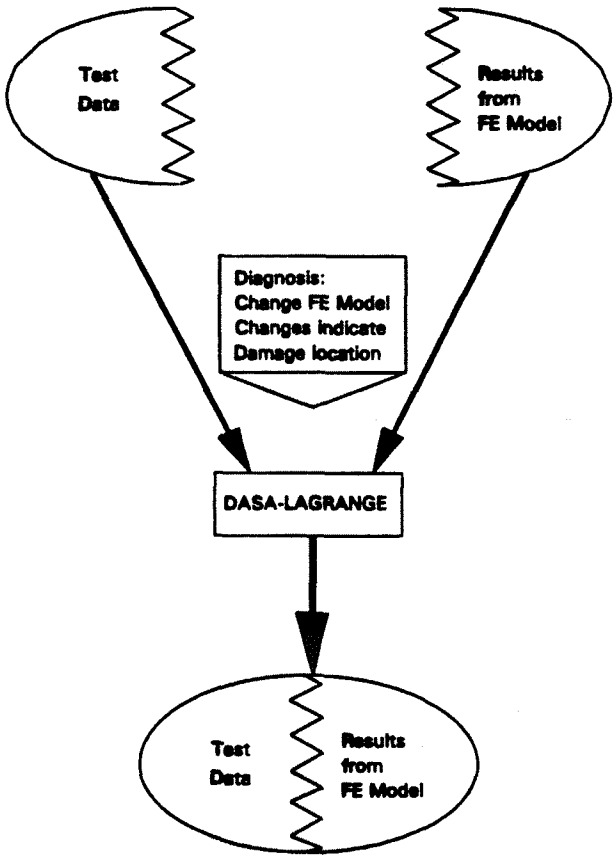

Fig. 1 Adaption of FE-Model to Test Data

Specifically the following method was applied:

Target function : Minimum changes of the FE-model.

Constraints : :

a) limited deviations of eigenvalues.

$$|\lambda_j - \lambda_{j,M}| \leq \epsilon \text{ (EPS)}$$

λj = jth eigenvalue

$\lambda_{j,M}$ = measured eigenvalue

b) limited deviations of eigenmode components

$$|\phi_{ij} - \phi_{ij,M}| \leq \epsilon \text{ (EPS)}$$

ϕ_{ij} = jtheigenmode, element i

$\phi_{ij,M}$ = measured eigenmode, element i

The "**Lagrange**" computer code [1] of Deutsche Aerospace was utilized to perform the numerical simulations which are presented in this paper.
The structural optimisation system "**Lagrange**" allows the optimisation of homogeneous isotropic, orthotropic or anisotropic structures as well as fibre reinforced materials. With the simultaneous consideration of different requirements in the design of aircraft structures it is possible to reduce the number of iteration steps between design, analysis and manufacturing.

Based on finite element methods for structures and panel methods for aerodynamics, the analysis with sensitivity includes modules for static, buckling, dynamic, static aeroelastic and flutter calculations.

The optimisation algorithms consists of mathematical programming methods and an optimal criteria procedure.

1.1 Detailed Description of the method used

The major steps of the method are as follows:

a) Represent a structured aircraft component with a finite element model.

b) Compare eigenvalues and eigenmodes of this FE-model with results of a ground resonance test on the new (i.e. undamaged) aircraft.

c) Update the FE-model with results of b, if necessary.

d) Choose your design variables by selecting parameters relating to finite elements in the area where structural damage is expected.

e) Measure components of the eigenmode vectors for the possibly damaged aircraft at selected nodal points of the FE Model for a number of eigenmodes at predefined maintenance cycles.

f) Plot the results of the Lagrange program as the model is adjusted minimising the structural changes to match the modes and frequencies of the damaged aircraft. Ideally, changes to the structure should occur where damage has happened and they are plotted as percentages of the original sizes.

2. Analysis and Test on a Defected Cantilever Beam

In order to validate the method, cantilever beams were used in the analysis and tests were carried out to prove that a finite element model can represent the dynamic behaviour of a test article. Three aluminium beams were fabricated to the dimensions shown in Figure 2.

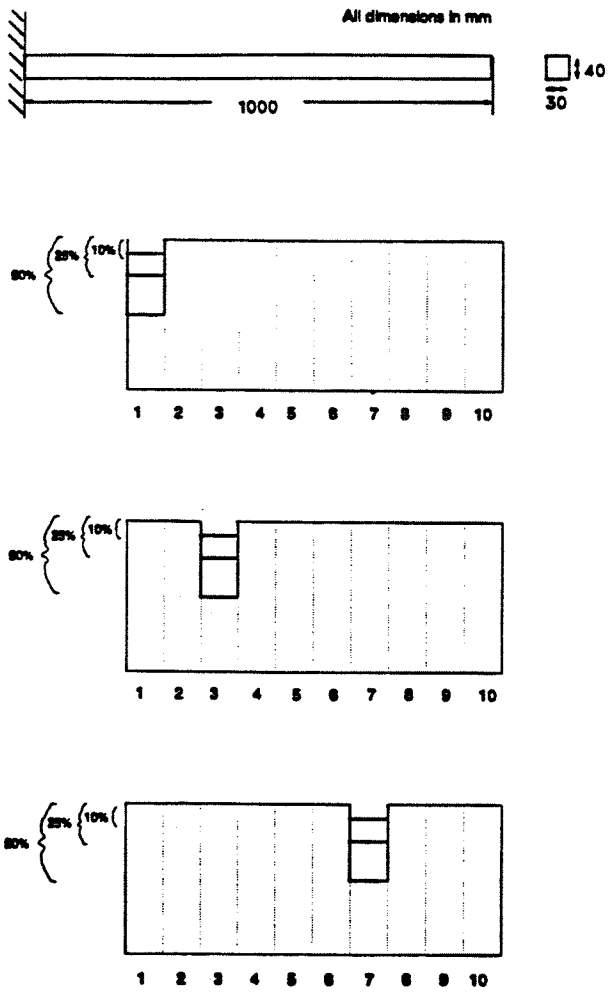

Fig. 2 Investigated Defected Beams

These beams were successively milled down at elements 1, 3 and 7 by 10%, 25% and 50% of their thickness and clamped as cantilevers. In order to determine the sensitivities of these beams, vibration modes and frequencies corresponding to the "simulated defects" were calculated for each cantilevered beam. The expression "simulated defects" is used because the defect is introduced on one finite element of the beam and does not represent a real defect such as a crack whose stiffness would be nonlinear due to the gap closing or opening. The finite element model consisted of 10 simple beam elements having a constant cross-sectional area and second moment of area. Only vertical bending was allowed (z,θ_x). Node 1 was constrained in all degrees of freedom.

2.1 Comparison of test and analysis results.

Eigenvector tests were performed with steady state sinusoidal excitation and a roving accelerometer and for all defected beams showed good correlation between calculated and measured data as can also be seen in Table 1 where mode frequencies are presented. Therefore it was decided to use the analytical beam data throughout for defect location. To represent experimental scatter on measured data, noise was introduced on the analytical mode shapes.

3. Detection and Location of Defects

The "Lagrange" computer code was used for this purpose. No updating of the model was performed since correlation between measured and calculated vibration data was good. For more complicated structures such an update may be required since this establishes the "no defect" situation. The vibration amplitudes of the defected beam in two locations, 4 and 7 were used as input data (constraints) for the computer code.

3.1 Sensitivity Study

A sensitivity study was performed in order to establish the level of damage and at which beam location this could be detected with the computer code. The parameters investigated were the number of input modes and the error between these modes and those which resulted from the updating, modal matching process called EPS (ϵ).

To define the deviations from the dimensions of the given beam with those calculated with the program using one number, the Euclidian norm Δ was used. Δ is the root mean square deviation from the ideal beam. The results of this evaluation are presented in Table 2 for various "cracks".

The use of frequencies only (first 4 frequencies) provides good identification, but the method is

Percent defect in element	0%	10%	25%	50%
1	I 0.97 II 0.98 III 0.96 IV 0.93	0.95 0.99 0.99	0.96 0.98 1.00	1.0 0.99 0.98
3	I 0.97 II 0.98 III 0.96 IV 0.93	0.94 0.96 0.96	0.95 0.95 0.95	0.96 0.92 0.94
7	I 0.97 II 0.98 III 0.96 IV 0.93	0.94 0.95 0.95	0.94 0.93 0.94	0.94 0.93 0.95

Table 1 Relative Difference of Eigenfrequencies $\frac{f_{measurement}}{f_{analysis}}$ for Modes I, II, III.

Number of measured modes m		Element 1 crack		Element 3 crack			Element 7		
		10%	25%	10%	25%	50%	10%	25%	50%
		RMS ERROR (Δ) in [%]							
4 frequencies m = 0		2.67	4.49	3.56	4.73	2.74	3.29	5.62	15.52
m = 1	ε = 5%	2.83	3.51	4.76	9.15	3.86	failed	failed	20.2
	ε = 1%	2.1	3.11	4.23	6.93	1.73	failed	10.26	25.6
m = 2	ε = 5%	2.72	2.93	4.44	8.58	3.82	4.14	12.65	2.63
	ε = 1%	1.26	1.52	4.42	6.52	2.14	3.46	1.41	1.95
	ε = 0.1%						2.79	2.85	3.74
m = 3	ε = 5%	2.67	3.52	4.05	4.93	2.98	4.29	7.33	3.0
	ε = 1%	1.18	1.05	3.29	3.83	3.05	2.74	2.51	5.32
m = 4	ε = 5%	2.21	2.39	3.0	3.69	3.54	3.24	4.39	2.90
	ε = 1%	0.84	1.18	1.97	4.39	4.27	1.82	3.00	3.1

Table 2 Results of a sensitivity study (RMS Δ errors as a function of number of modes)

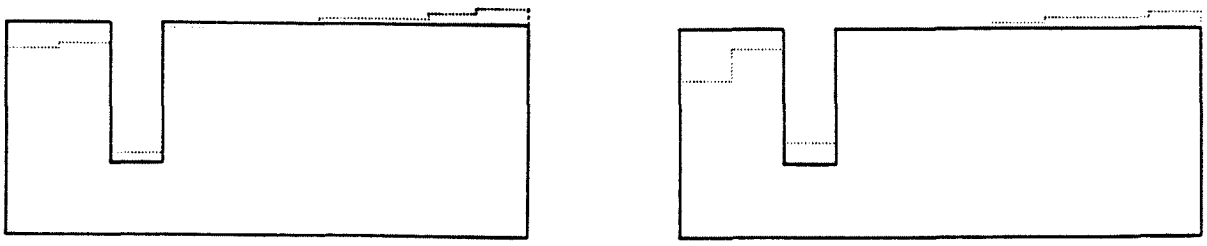

a. Identification with First Mode and Frequency (No Noise on Input Data)

b. Identification with First Mode and Frequency (14% Variance on Input Data)

Fig. 3 The Influence of Noise on Input Data (50% Crack In Element 3)

restricted to beam like structures with bending modes only. If modes exist in the adapted frequency range which contain other degrees of freedom executed via a "crack", a change of modes could occur and the method would not know which modes to adapt.
For crack identification on aeroplanes the method using modes and eigenfrequencies is recommended. As is shown, two to three modes at two locations can identify "cracks" as low as 10% on all span-wise positions for beam like structures, found in commercial and military transport aircraft wings.
The requirement ϵ (EPS) which is the relative error on fitting the mode shapes can also be interpreted as the required accuracy to measure mode shapes. The results obtained indicate that $\epsilon = 5\%$ is a reasonable value for "crack" identification in simple cantilever beams. In general, mode shapes can be measured with such an accuracy assuming they are not closely spaced in frequency.

3.2 Sensitivity to noise on the input data

In order to assess the sensitivity of the method to measuring errors in the input data a limited number of calculations were performed with simulated noise on the data. As an example in figure 3 a 50% crack in element 3 can be detected with 14% variance on the input data (measured amplitudes).

4. Analysis of a Carbon Fibre Composite (CFC) Fin and a Rudder with a Defect

The next step to test the method was to examine a plate structure, in this case a fin of a predecessor of the European Fighter Aircraft. Mode shapes now become more complicated because torsion modes are occurring. Since the fin also has a rudder attached to it, vibration modes exist which are dominated by rudder motions. In order to save weight, 70% of the aircraft surface area is fabricated from CFC including the fin and rudder.
Vibration modes and frequencies were calculated using the analysis part of the "Lagrange" code. These modes and frequencies were compared with modes and frequencies measured on a dynamically scaled 1:5 model of the fin made as a replica also from CFC. Since correlation was good it was deduced, that the FE-model is a good representation of the real fin structure and could be used, as a first approach, to simulate defects by changing skin thicknesses of this FE-model. The eigenmodes and -frequencies of this modified FE-model were used instead of real test data of a fin which had these built in defects. Design variables were also the changed skin thicknesses which is a very limited case. In reality all the finite elements of the fin, in this case 188 elements, would have to be design variables since the defect location is unknown. The cost of the computer time for this effort was too high and such an investigation has to be performed on a project study.
A finite element model of the fin and rudder structure was generated and the following types of elements were used:

- pin jointed bar, called ROD
- linear triangular plate element (in plane forces only) called TRIA3
- linear rectangular plate element (in plane forces only) called QUAD4

The structural elements are plotted in figure 4 for the right skin and for the substructure (ribs and spars). Each main fin box skin element consists of a four layer CFC laminate. The fin tip is idealized as quasi-isotropic Glass Fibre Composite (GFC) which means that it contains equal amounts of glass fibres in the four direction angles, 0°, +45, -45°, 90°. The total number of elements used is 188.

4.1 Calculation of Eigenvectors and Natural Frequencies

Three sets of eigenvectors and natural frequencies of the fin were calculated, using the FE-model described:

a Eigenvectors for Fin and Rudder without a Defect

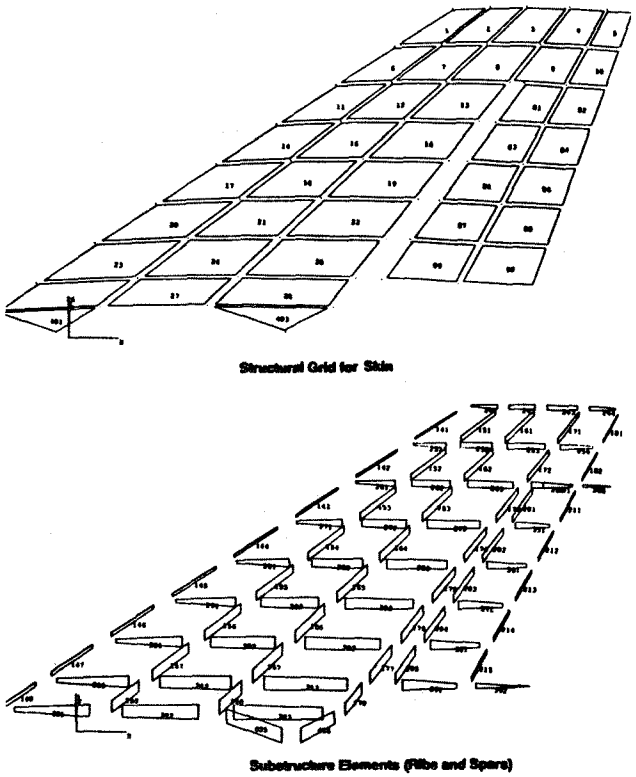

Fig. 4 Structural Grid for Fin

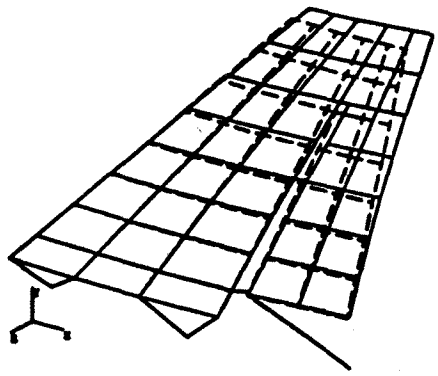

Fin First Bending (f = 11.2Hz)

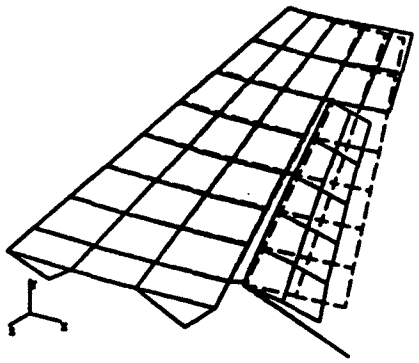

Rudder Yaw (f = 33.2Hz)

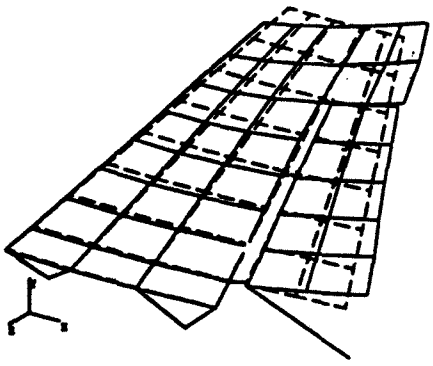

Fin First Torsion (f = 41.3Hz)

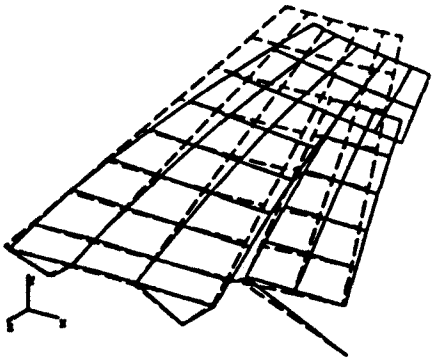

Fin Tip Torsion I (f = 56.4Hz)

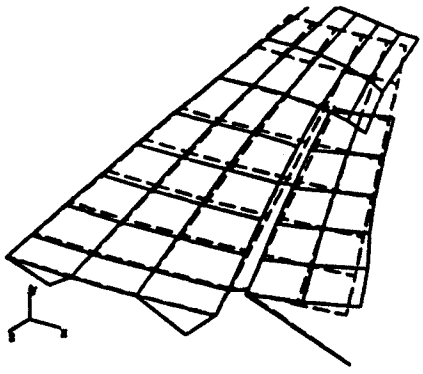

Fin Tip Torsion II (f = 66.9Hz)

Fig. 5 Mode Shapes of Fin and Rudder without a Defect

The mode shapes for this case are shown in figures 5. Clearly the first three modes can be identified respectively as fin bending, rudder yaw and fin torsion. The two higher frequency modes are characterized by large fin tip motions which are related to the much lower modulus of elasticity of the GFC fin tip material (about 12% of CFC). A comparison is made with results from a Ground Resonance Test (GRT) on the full aircraft in Table 3 which shows good correlation of modal frequencies considering that the fin is connected to the fuselage and not clamped as in the FE model. This clamping increases fin bending mode frequency.

The rudder yaw stiffness was underestimated (hydraulic actuators were stiffer than assumed in the FE model) which in turn reduces the aircraft fin torsion modal frequency due to the coupling effect of the rudder on the fin. From Table 3, considering the differences in the parameters of the aircraft GRT and the FE-model it can be said that the analytical model predicts the dynamic behaviour of the aircraft well.

b Eigenvectors for Fin and Rudder with a Simulated Defect in the Fin Skin

The fin skin elements 20 to 28 (see figure 4) were reduced to 50% of their original value. A vibration analysis was performed with the modified FE-model and the eigenvalues and eigenvectors were calculated.

The modal frequencies for this case are compared with the frequencies for the fin with and without a defect in Table 4.

MODE NUMBER	MODE DESCRIPTION	FE-MODEL [Hz]	A/C-GRT [HZ}
1	First Fin Bending	11.2	10.6
2	Rudder Yaw	33.2	37.5
3	Fin Torsion	41.3	32.6
4	Tip Torsion 1	56.4	48.7
5	Tip Torsion II	66.9	72.8

Table 3 Comparison of the Modal Frequencies the FE-Model and the Full A/C-GRT

MODE NUMBER	MODE DESCRIPTION	No Fin Defect [Hz]	Fin Defect [Hz]
1	First Fin Bending	11.2	9.8
2	Rudder Yaw	33.2	32.9
3	Fin Torsion	41.3	38.9
4	Tip Torsion 1	56.4	47.3
5	Tip Torsion II	66.9	66.4

Table 4 Comparison of the Modal Frequencies with and without Defect

MODE NUMBER	MODE DESCRIPTION	NO RUDDER DEFECT [HZ]	50% RUDDER ATTACHMENT STIFFNESS [Hz]
1	First Fin Bending	11.2	11.2
2	Rudder Yaw	33.2	26.9
3	Fin Torsion	41.3	40.6
4	Tip Torsion I	56.4	56.5
5	Tip Torsion II	66.9	66.2

Table 5 : Comparison of Modal Frequencies with and without Rudder Attachment Defect

This shows that relatively small frequency reductions occur for a large change in fin skin thickness.

c Eigenvectors for the Fin and Rudder, with a Simulated Defect in the Rudder Yaw Stiffness.

This case was simulated by reducing the attachment stiffness to 50% of its original value.
The frequencies for this case are compared with the frequencies for the undamaged case in Table 5. It is interesting to note that only the rudder yaw modal frequency changes whilst all other frequencies stay almost the same. The rudder yaw modal frequency is reduced by less than would be expected from a stiffness drop of 50%.

4.2 Detection and Localisation of Defect

Two defect conditions were considered for the finite element model:

a) A reduction of the fin skin elements 20 to 28 to 50% of their original thicknesses.
b) A reduction of the rudder attachment stiffness to 50%.

Damage detection could be achieved for the first case when the first mode was constrained with an EPS of 1% on all nodal point amplitudes. This is shown in Figure 6.

The second case, Defect on the Rudder Yaw attachment, could be detected very well as can be seen in figure 7 where 4 design variables are shown. Design variable 19 which is the attachment spring goes to 50% whilst all other design variables are unchanged.

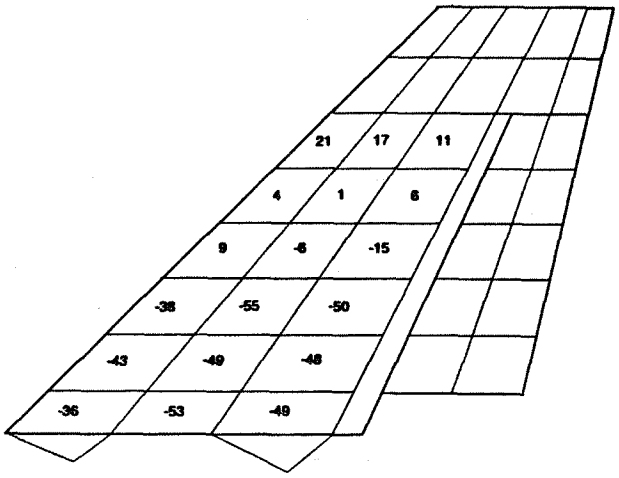

Fig. 6 Skin Thicknesses Updated as Percentages of Undefected (First Mode, EPS = 1%, All Amplitudes)

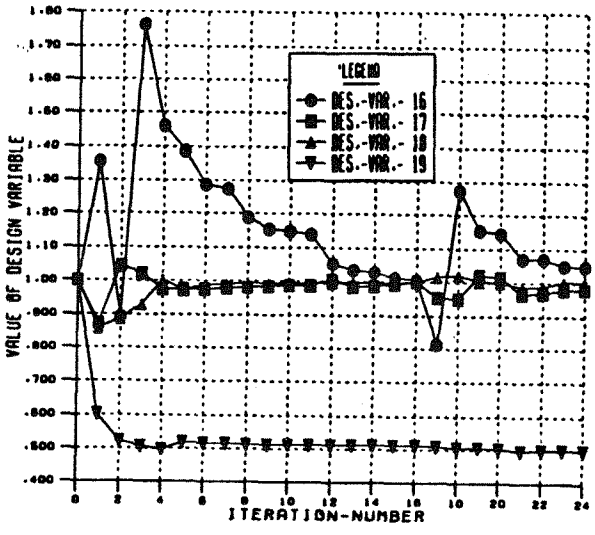

Fig. 7 Design Variable History (50% Damage on Rudder Attachment)

5. The use of neural networks for damage detection and location

Neural networks have been used lately to a large extent. One of the big advantages is that they do not require an analytical knowledge of the aircraft.

5.1 Cantilever Plate: Computation of the Training Data

A plate was modelled using the LUSAS Finite Element (FE) system. The material constants of aluminium were used and the dimensions chosen were 300mm x 200mm x 2.5mm; the built-in end was taken along one of the short sides. An aspect ratio of 1.5 was chosen. For the network training, it was decided to estimate the modeshapes and curvatures on a regular 4 x 4 grid and attempt to locate faults within the areas so defined. Faults were simulated by lowering the stiffness of the element, in this case the Youngs Modulus was reduced to 1 % of its usual value. For the purposes of network training, severity was varied by 'deleting' groups of elements rather than modulating the stiffness of a fixed element. This strategy clearly requires a high resolution for the mesh, so 20 x 20 elements were used. For each fault location, faults of three severities were simulated by deleting one, five (in a cross shape), or nine elements.

For the FE model, eight-node semi-loof elements were used, although this was rather time-consuming, the results justified the expenditure. The estimated natural frequencies were 23.5, 79.4, 146.2, 364.6 and 419.2 Hz, agreeing with reference 2 to well within its stated confidence interval. The curvature estimation required a little thought; for a beam for example, the second derivative of the modeshape would be a sufficient approximation. However, as the modal displacements ψ for a plate is a function of both x and y (assuming standard Cartesian coordinates), the derivative is replaced by a gradient vector.

$$\underline{\nabla}\psi = \left(\frac{\partial\psi}{\partial x}, \frac{\partial\psi}{\partial y}\right)$$

As some scalar analogue of the curvature is still required for training, the following quantity was chosen

$$\kappa = \| \underline{\nabla} \cdot \| \underline{\nabla}\psi \| \|$$

where

$$\|\underline{\nabla}\psi\| = \sqrt{\left(\frac{\partial\psi}{\partial x}\right)^2 + \left(\frac{\partial\psi}{\partial y}\right)^2}$$

explains the use of the norm $\| \|$. A simple centred difference was used to estimate the partial derivatives. In order to amplify the disturbance due to the fault, the curvatures corresponding to the undamaged state are subtracted throughout. The curvature information is available from experiment.

5.2 Results

The measurements of the network inputs were taken at the nodes of the dashed grid in Figure 8. One output was associated with each fault location (the numbered points in Figure 8). A Multi-Layer Perceptron (MLP) (Reference 2) network with a single hidden layer was used; the final network structure

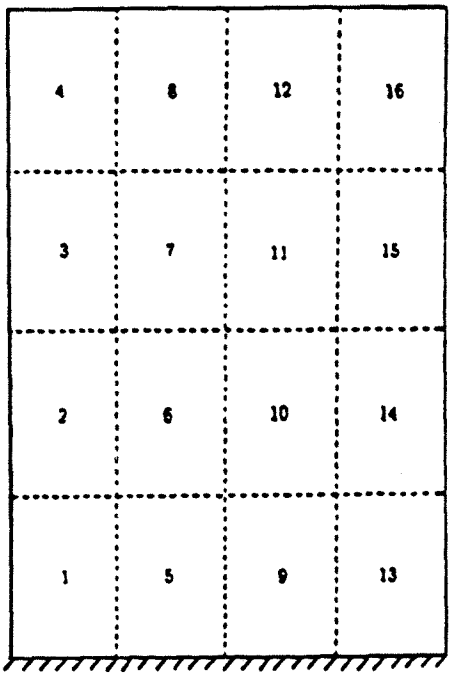

Fig. 8 Location of Faults

being 20:18:16. Note that with this indexing system, the outputs associated with the free end of the plate are 4, 8, 12 and 16; it was anticipated that the diagnostic networks would have most difficulty with faults in this area. The networks were trained to respond in proportion to the severity of the fault, in this case the area of damage; the desired outputs were taken to be 0.1, 0.5 and 1.0 for the three levels of damage.

The diagnostic network is used in the following way: when a curvature pattern is presented, the highest of the outputs is taken to signal the fault

Fault element	Output node															
	1	2	3	4	5	6	7	8	9	10	11	12	13	14	15	16
1	X	-	-	-	-	-	-	-	-	-	-	-	-	-0.1	-	-
2	-	X	-	-	-	-	-	-	-	-	-	-	-	-	-	-
3	-	-	X	-	-	-	-	-	-	-	-	-	-	-	-	-
4	-	-	-	X	-	-	-	-	-	-	-	-	-	-	-	-
5	-	-	-	-	X	-	-	-	-	-	-	-	-	-	-	-
6	-	-	-	-	-	X	-	-0.2	-	-	-	-	-	-	-	-
7	-	-	-	-	-	-	X	-	-	-	-	-	-	-	-	-
8	-	-	-	-	-	-0.1	-	X	-	-	-	-	-	-	-	-
9	-	-	-	-	-	-	-	-	X	-	-0.1	-	-	-	-	-
10	-	-	-	-	-	-	-	-	-	X	-	-0.2	-	-	-	-
11	-	-	-	-	-	-	-	-	-0.1	-	X	-	-	-	-	-
12	-	-	-	-	-	-	-	0.1	-	-0.1	-	X	-	-	-	-
13	-	-	-	-	-	-	-	-	-	-	-	-	X	-	-	-
14	-0.2	-	-	-	-	-	-	-	-	-	-	-	-	X	-	-
15	-	-	-	-	-	-	-	-	-	-	-	-	-	-	X	-
16	-	-	-	-	-	-	-	-	-	-	-	-	-	-	-	X

Table 6 Location Matrix from Network Trained on First Modeshape Curvature

location i.e. if output 6 is highest, it is assumed that the element corresponding to output 6 is damaged. A simple measure of the network accuracy is provided by the location matrix which is defined as follows. The average response of each output i = 1, ..., 16 is taken when all patterns corresponding to a given fault location j = 1, ..., 16 are presented in the order described above. The set of averages is then scaled so that the largest is unity and the numbers are entered into the j^{th} row of the matrix. It is clear that a perfectly trained network will produce in this way the unit matrix. Table 6 shows the location matrix for the network described above. The zero elements of the matrix are shown as dashes and the unit elements as crosses to improve the clarity of the results.

Looking at the results in Table 6 one can see that this is a successful diagnostic network. The fault location is always correct. There are no particular problems associated with elements at the free end. Consideration of the network outputs over the training sets showed that all faults including the lowest fault were sized correctly.

6. Dynamic Test Methods for Aircraft Structures

A large number of vibration responses can be acquired by scanning over a surface with a laser vibrometer and employing modal analysis with stochastic excitation signals to keep testing time to a minimum.
Modern aeroplanes have hydraulic systems and actuators installed to actuate their flight control surfaces which is commanded and controlled by electrical signals (fly by wire). Therefore it is possible to stimulate the control surfaces with a repeatable signal - such as a frequency sweep or random noise - for a short period of time and obtain repeatable data. This Built In Equipment (BITE) can also be cleared by the aircraft manufacturer so that no structural damage can occur due to mishandling of the system.
In this section, examples are shown, presenting evidence that hydraulic actuators produce forces above their specified frequency range (which is below 5 Hz) and that there are peaks in the frequency response functions of primary surfaces, excited by these actuator forces which can be recognised as responses of vibration modes identified in a separate ground resonance test. An application of using built-in hydraulic actuators to excite vibration modes of fighter aeroplanes is given in [4]. Aircraft Ground Vibration Tests (GVT) are usually performed by means of the classical technique of eigenmodes isolation. Sinusoidal excitation signals are applied to the structure using sets of external electrodynamic shakers, the forces of each of which being adjusted in order to achieve the separation of the different eigenmodes, one after the other.

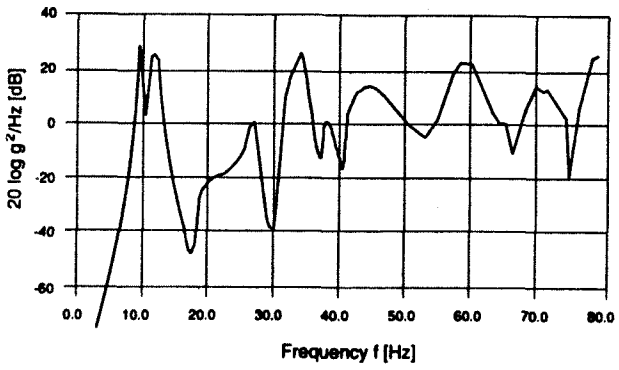

Fig. 9 Fin Tip Acceleration

In recent years, the manufacturers of aircraft equipped with "fly-by-wire" control systems test structural frequency response from control surface excitation to check the stability of the closed loop system. This frequency response can be exploited to yield structural mode shapes and frequency information.

A test was performed in order to assess the level of coupling of structural vibration modes with the flight control system on a fighter aircraft. During these tests, vibration signals were injected into the flight control system which resulted in motion of the flight control surfaces (in this case the outboard flaps). These surfaces produced mass and inertia forces which in turn excited the aircraft's primary surfaces. The power spectral density of the fin acceleration measured with a tip mounted accelerometer is shown in Figure 9. Two distinct peaks can be seen at 10.55 Hz and 12.11 Hz. Modes for these frequencies are shown in figure 10. These modes could be used for damage detection.

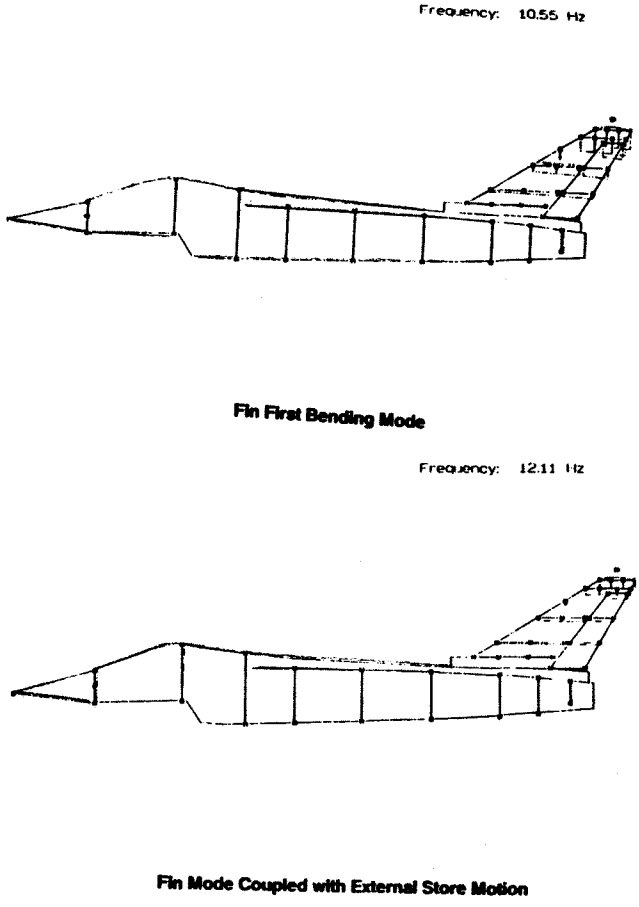

Fig. 10 Fin Mode Shapes

References

1. Krammer, J., "Practical architecture of design optimisation software for aircraft structures taking the MBB-Lagrange Code as an example", AGARD-LS-186, May 1992.
2. Leissa, A.W., Journal of Sound and Vibration, Vol. 31, 1973, pp.257-293.
3. Rumelhart, D.E., and McClelland J.L., "Parallel Distributed Processing: Explorations in the Microstructure of Cognition", (Two Volumes), MIT Press, 1988.
4. Gravelle, A., Lepart, M., Lubrina, "Aircraft Ground Vibration Test by Means of Flight Control Surfaces", ONERA, International Forum on Aeroelasticity and Structural Dynamics, Aachen, June 1991.